Available online at www.sciencedirect.com
SCIENCE DIRECT®
International Journal of Mass Spectrometry 241 (2005) 109–117
International Journal of Mass Spectrometry
www.elsevier.com/locate/ijms

Binding interactions of mono- and diatomic silver cations with small alkenes: experiment and theory

Manuel J. Manard, Paul R. Kemper, Michael T. Bowers*

Department of Chemistry and Biochemistry, University of California, Santa Barbara, CA 93106, USA

Received 4 November 2004; accepted 6 December 2004
Available online 9 January 2005

Abstract

Temperature-dependent equilibrium methods were used to measure sequential association energies and entropies for the attachment of C_2H_4 and C_3H_6 ligands to ground-state $Ag^+(^1S, 4d^{10})$ and $Ag_2^+(^2\Sigma_g, 4d^{20}\ \sigma(5s)^1)$. Experimental bond dissociation energies (BDEs) of $Ag^+(C_2H_4)_n$ are 32.2, 30.1, 13.6, 6.5 and 4.4 kcal/mol for $n = 1$–5, respectively, with the BDE of the sixth ligand estimated to be 3.3 kcal/mol. The BDEs of $Ag_2^+(C_2H_4)_n$ are 24.7, 22.5, 12.5, 7.7 and 2.9 kcal/mol for $n = 1$–5, respectively. The BDEs of $Ag^+(C_3H_6)_n$ are 39.2, 32.9, 13.3, 7.0 and 3.0 kcal/mol and the BDEs of $Ag_2^+(C_3H_6)_n$ are 28.1, 25.8, 12.4, 9.3 and 4.2 kcal/mol for $n = 1$–5, respectively. A first solvation shell of four is observed for the attachment of both C_2H_4 and C_3H_6 ligands to both the Ag^+ and Ag_2^+ core ions with all subsequent ligand additions taking place in the second solvation shell. Electronic structure calculations at the DFT-B3LYP level were performed in order to determine the vibrational frequencies, rotational constants and geometries of all the observed Ag^+ and Ag_2^+ clusters as well as the nature of the bonding of these clusters and its variation with core ion coordination.

Keywords: Silver cations; Alkene; Bond dissociation energy; Density functional theory

1. Introduction

The interactions between transition metals and small molecules have been the source of extensive study [1]. One of the underlying reasons is that transition metals have proven to be essential components in a number of catalytic reactions. Systematic experiments have examined the properties of an assortment of gas-phase metal ion M_y^+–X_n clusters with X = H_2 [2–12], CO [3–18], O_2 [19,20], and CH_4 [3,21–24] along with a variety of other ligands [25–29]. These experiments, coupled with theoretical calculations, have broadened our understanding of the nature of transition metal ion bonding and have provided some of the fundamental information that is necessary to elucidate the complex factors involved with many catalytic processes.

Recently, considerable attention has been paid to silver clusters and their interactions with small, unsaturated hydrocarbons. This interest is due in part to the discovery that silver clusters on semiconductor surfaces serve as epoxidation catalysts for ethene and propene [30]. Numerous experimental and theoretical investigations have been conducted in order to ascertain the nature of the interaction between silver and these small alkenes [31–37]. Despite the considerable amount of study that has been given to these systems, many interesting questions still remain. It is well known that bulk-phase silver is chemically inert, yet nanoscale particles exhibit catalytic properties. This leads directly to questions such as what size silver clusters, or range of sizes, are responsible for catalysis and where does the transition from nano to bulk properties take place. Investigations into the relative energetics of silver clusters interacting with various species that participate in the catalytic reaction, such as C_2H_4, C_3H_6, and O_2, could provide important information toward answering these questions.

* Corresponding author. Tel.: +1 805 893 2893; fax: +1 805 893 8703.
E-mail address: bowers@chem.ucsb.edu (M.T. Bowers).

1387-3806/$ – see front matter © 2004 Published by Elsevier B.V.
doi:10.1016/j.ijms.2004.12.007

Dewar initially proposed an interaction model to interpret the structure of metal–olefin complexes [38]. This model suggests that bonding consists mainly of electron density donated from the π-orbitals of the ligand to the unoccupied s-orbital of the metal coupled with back-donation from the filled d-orbitals of the metal to the unoccupied π*-orbitals of the ligand. Subsequent studies have used this model to explain the bonding of small alkenes to group 11 transition metal cations [32,33,35]. Furthermore, it has been shown that back-donation plays a more significant role in the bonding of first row transition metals and is less important for the second and third row counterparts [35–37].

In this work, temperature-dependent equilibrium measurements in conjunction with ab initio calculations were used to determine the binding interactions of $Ag^+(4d^{10})$ and $Ag_2^+(4d^{10}\ \sigma(5s)^1)$ clustering with C_2H_4 and C_3H_6, respectively. Some of these systems have been previously investigated in other laboratories. Guo and Castleman [32] measured the binding energies of one and two C_2H_4 ligands to Ag^+. Chen and Armentrout [31] examined reactions of Ag^+ with a variety of small hydrocarbons and reported a lower limit for the BDE of the $Ag^+(C_2H_4)$ ion. Little information exists in the literature for $Ag^+(C_3H_6)$ clusters, and no prior studies could be found on Ag_2^+ interactions with either C_2H_4 or C_3H_6. Of particular interest is the nature of the bonding between these Ag clusters and the alkene ligands. The relative strength of the bonds corresponding to the early ligand additions compared to that of the later additions as well as the comparisons between analogous $Ag^+(L)_n$ and $Ag_2^+(L)_n$ clusters could provide insight into the characteristics of the silver–alkene bond. Additionally, this initial investigation should prove a useful starting point for the study of the interactions of larger silver clusters with ethene and propene.

2. Experimental methods

A description of the instrument and experimental details has been given previously [5,7,39], and only a brief description will be given here. The silver ions are generated by pulsed laser vaporization of a translating/rotating silver rod in a high-pressure Ar bath gas. Sliver clusters exiting the source are then mass selected by a quadrupole mass filter and injected into a 4-cm long drift/reaction cell containing a mixture of reactant gas (either C_2H_4 or C_3H_6) and He. The typical composition of the gas mixture is 4.5 Torr of He combined with 0.01–0.5 Torr of either C_2H_4 or C_3H_6. Equilibria (Eq. (1) where $m = 1$–2 and L = C_2H_4 or C_3H_6) are quickly established as the various silver–alkene clusters are drawn through the cell under the influence of a small electric field:

$$Ag_m{}^+L_{n-1} + L \rightleftarrows Ag_m{}^+L_n \tag{1}$$

The electric field is small enough so that the thermal energy of the ions is not significantly perturbed. The clusters exiting the cell are then mass selected by a second quadrupole and detected.

Integrated peak areas are recorded and these values, along with the pressure of the ligating gas (P_L) in Torr, are used to determine an equilibrium constant (K_p°) for each reaction using Eq. (2):

$$K_p^\circ = \frac{[Ag_m{}^+L_n]}{[Ag_m{}^+L_{n-1}]}\frac{760}{P_L} \tag{2}$$

The equilibrium constants can then be used to calculate the standard Gibbs free energies for the reactions:

$$\Delta G_T^\circ = -RT\ln(K_p^\circ) \tag{3}$$

and the values obtained for ΔG_T° plotted versus the temperature, to obtain ΔS_T° and ΔH_T° for each reaction using Eq. (4):

$$\Delta G_T^\circ = \Delta H_T^\circ - T\Delta S_T^\circ \tag{4}$$

The resulting plots are linear over the experimental temperature range for all systems reported here. A least squares-fitting procedure is used to obtain slopes and intercepts of each line. The slopes are used to determine the association entropy for Eq. (1) (ΔS_T°) and the intercepts give the corresponding ΔH_T° values. The reported uncertainty in these values is a measure of variance in the data from the fit. The 0 K BDE, $-\Delta H_0^\circ$, is then determined by fitting and extrapolating the data to 0 K using statistical thermodynamics. The necessary vibrational frequencies and rotational constants are taken from density functional theory (DFT) [40] calculations (see theory section). In all cases, vibrational frequencies are varied over a wide range, and the effect on ΔH_0° is included in the error limits. It should be stressed that uncertainties in these parameters have little effect on the final values of ΔH_0°. A thorough discussion of this fitting procedure and an estimation of the errors involved has been given previously [2,5].

3. Theory

The product ions discussed here were all examined theoretically to determine the molecular parameters needed to analyze the experimental data and to identify factors important in the bonding. DFT calculations were carried out using the B3LYP hybrid functional [41,42] and the Gaussian 98 package [43]. For all of the calculations reported here, carbon and hydrogen were described using the standard 6-31+G** basis set [44]. The basis set for silver is a (5s6p4d)/[3s3p2d] contraction of the Hay-Wadt ($n+1$) effective core potential (ECP) valence double zeta basis proposed by Hay [45,46]. Here, the outermost core orbitals are not replaced by the ECP, but are instead treated equally with the valence orbitals. This allows for increased accuracy in the calculations without a substantial increase in computation time. The ECP for silver incorporates the Darwin and mass–velocity relativistic effects into the potential.

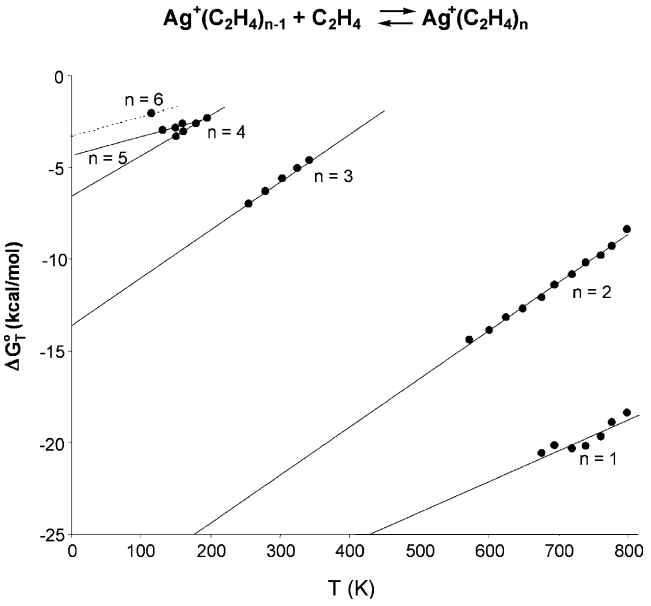

Fig. 1. Plot of experimental ΔG_T° vs. temperature for the association reactions $Ag^+(C_2H_4)_{n-1} + C_2H_4 \rightleftarrows Ag^+(C_2H_4)_n$. For $n = 6$, the slope of the line is the same as the $n = 5$ line.

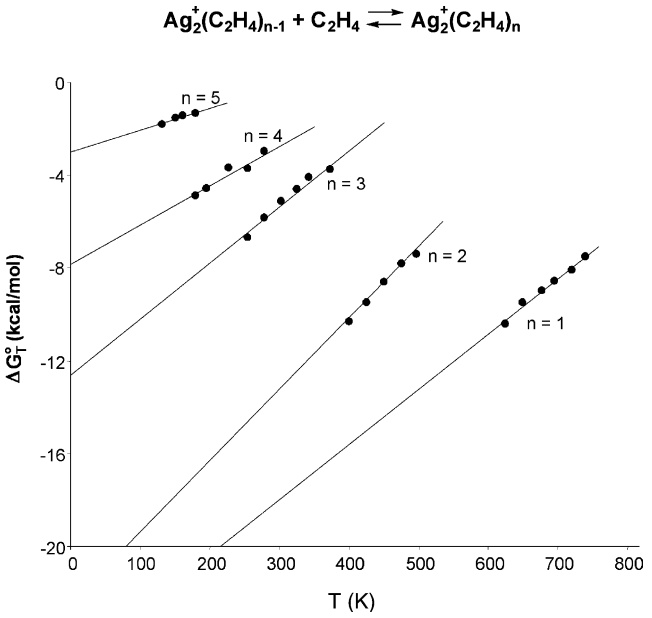

Fig. 2. Plot of experimental ΔG_T° vs. temperature for the association reactions $Ag_2^+(C_2H_4)_{n-1} + C_2H_4 \rightleftarrows Ag_2^+(C_2H_4)_n$.

Geometry optimizations of $Ag_{1,2}^+(C_2H_4)_n$ and $Ag_{1,2}^+(C_3H_6)_n$ clusters were performed over a wide variety of conceivable geometries in order to obtain minimum energy cluster conformations and to ensure that no alternative theoretical geometries exist that significantly differ from those reported here. All confirmed minima consist of largely unperturbed C_2H_4 and C_3H_6 ligands bound to a metal core ion.

4. Results

A plot of ΔG_T° versus T for addition of up to six C_2H_4 ligands to Ag^+ is given in Fig. 1 and a plot of ΔG_T° versus T for addition of up to five C_2H_4 ligands to Ag_2^+ is given in Fig. 2. The slopes and intercepts of the lines yield the ΔH_T° and ΔS_T° values given in Table 1 for the $Ag^+(C_2H_4)_n$ system and in Table 2 for the $Ag_2^+(C_2H_4)_n$ system. ΔH_0° values obtained as previously described are also listed in Tables 1 and 2 for the respective silver–ethene systems. Procedures identical to those used for the ethene clusters were used to obtain ΔH_T°, ΔS_T°, and BDEs for the propene clusters. The experimental data are given in Fig. 3 for the $Ag^+(C_3H_6)_n$ system and in Fig. 4 for the $Ag_2^+(C_3H_6)_n$ system. All measured thermodynamic quantities are reported in Tables 3 and 4 for the $Ag^+(C_3H_6)_n$ and $Ag_2^+(C_3H_6)_n$ systems, respectively. Additionally, theoretical binding energies calculated for all of the observed silver–alkene clusters are listed in Tables 1–4 and structures obtained from DFT calculations are given in Figs. 5 and 6 for the silver–ethene systems and in Figs. 7 and 8 for the silver–propene systems.

Several trends in the experimental data were observed. First, in each of the four systems studied, clusters with at least five ligands were observed at the temperatures accessible in our experiments. For the Ag^+/C_2H_4 system, addition of a sixth ligand was also detected. Second, similarities in the BDEs were observed. The strongest bond in each of the four systems results from the addition of the first alkene ligand to either Ag^+ or Ag_2^+, with values ranging from 24.7 kcal/mol for $Ag_2^+(C_2H_4)$ to 39.2 kcal/mol for $Ag^+(C_3H_6)$. In all cases, the second ligand is bound several kcal/mol more weakly than

Table 1
Data summary for $Ag^+(C_2H_4)_{n-1} + C_2H_4 \rightleftarrows Ag^+(C_2H_4)_n$

n	Experiment				Theory	
	$-\Delta H_T^\circ$ (kcal/mol)	$-\Delta S_T^\circ$ (cal/mol K)	$-\Delta H_0^\circ$ (kcal/mol)	T[a]	D_e (kcal/mol)	D_o (kcal/mol)
1	32.5 ± 2.5	18.9 ± 4	32.2 ± 3.0	675–800	32.53	31.24
2	30.3 ± 0.8	27.5 ± 1	30.1 ± 1.3	500–800	27.59	26.10
3	14.0 ± 0.6	27.0 ± 2	13.6 ± 0.8	255–345	10.42	9.10
4	6.8 ± 0.4	21.9 ± 2	6.5 ± 0.8	160–195	3.61	2.85
5	4.5 ± 0.5	11.3 ± 3	4.4 ± 0.6	130–160	–	–
6	–	–	∼3.3[b]	115	–	–

[a] Temperature range over which equilibrium data was acquired, in kelvin.
[b] Estimate (see text).

Table 2
Data summary for $Ag_2^+(C_2H_4)_{n-1} + C_2H_4 \rightleftarrows Ag_2^+(C_2H_4)_n$

n	Experiment				Theory	
	$-\Delta H_T^\circ$ (kcal/mol)	$-\Delta S_T^\circ$ (cal/mol K)	$-\Delta H_0^\circ$ (kcal/mol)	T[a]	D_e (kcal/mol)	D_o (kcal/mol)
1	25.1 ± 1.5	23.8 ± 2	24.7 ± 2.0	625–740	22.14	20.86
2	22.7 ± 1.3	31.0 ± 3	22.5 ± 1.8	400–500	17.40	16.19
3	12.9 ± 0.7	25.3 ± 3	12.5 ± 1.0	255–375	8.93	7.82
4	8.1 ± 0.4	18.2 ± 2	7.7 ± 0.6	180–280	5.54	4.57
5	3.1 ± 0.6	10.1 ± 3	2.9 ± 0.8	130–180	–	–

[a] Temperature range over which equilibrium data was acquired, in kelvin.

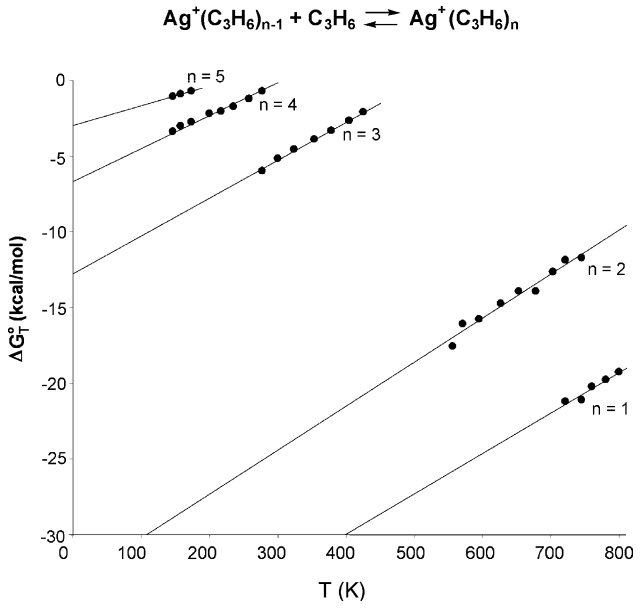

Fig. 3. Plot of experimental ΔG_T° vs. temperature for the association reactions $Ag^+(C_3H_6)_{n-1} + C_3H_6 \rightleftarrows Ag^+(C_3H_6)_n$.

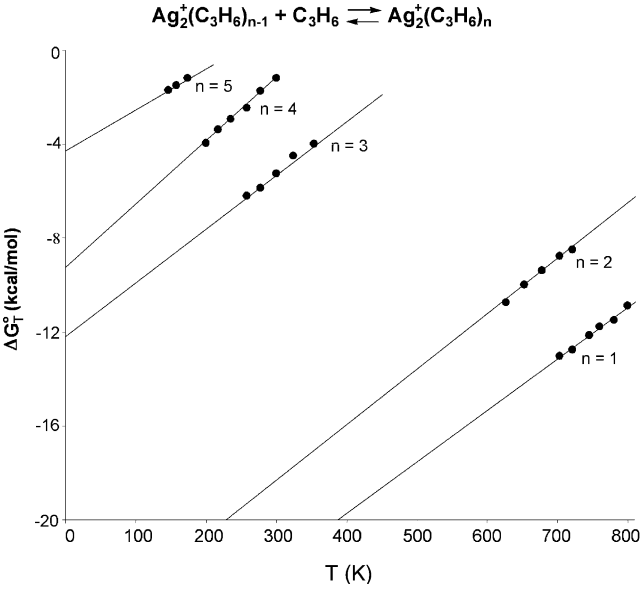

Fig. 4. Plot of experimental ΔG_T° vs. temperature for the association reactions $Ag_2^+(C_3H_6)_{n-1} + C_3H_6 \rightleftarrows Ag_2^+(C_3H_6)_n$.

the first. Furthermore, each of the first two C_3H_6 ligands bind more strongly than C_2H_4 to both Ag^+ and Ag_2^+ by several kcal/mol. Between the second and third ligands, there is a substantial drop in the BDEs of 10–20 kcal/mol. Each additional ligand in all four systems is bound more weakly, with the fifth (and sixth in the case of the Ag^+/C_2H_4 system) bound by less than 5 kcal/mol.

Similarities in the association entropies for the four systems can also be seen. For the additions of the first four

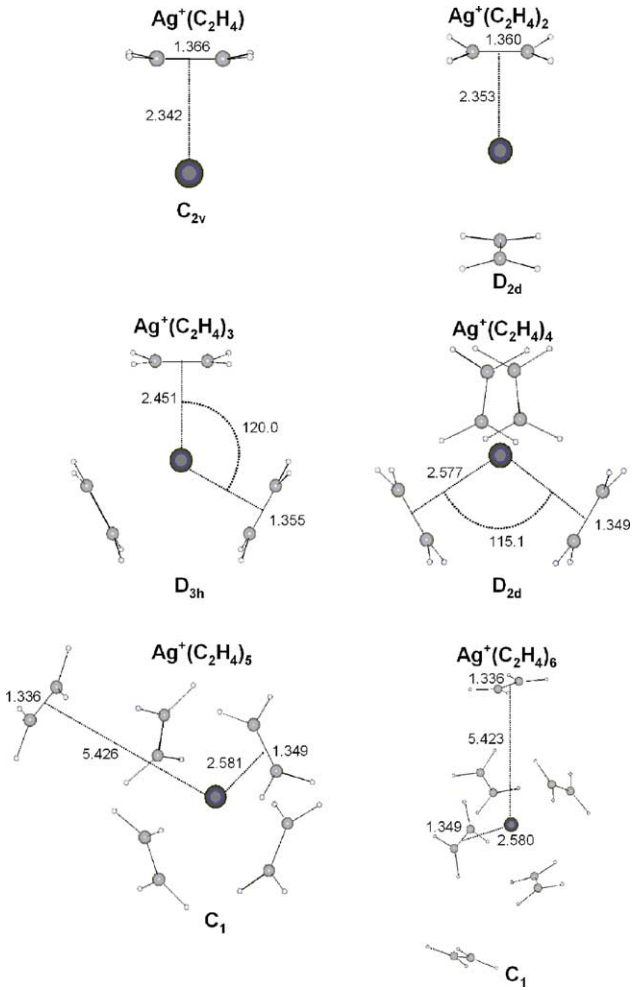

Fig. 5. Theoretical geometries of the $Ag^+(C_2H_4)_n$ clusters calculated at the DFT B3LYP level. Distances are in angstroms and angles in degrees. The z-axis is taken as the Ag^+—C_2H_4 bonding axis. All Ag^+—C_2H_4 bond distances are measured from the Ag^+ ion to the center of the C—C double bond.

Table 3
Data summary for $Ag^+(C_3H_6)_{n-1} + C_3H_6 \rightleftarrows Ag^+(C_3H_6)_n$

n	Experiment				Theory	
	$-\Delta H_T^\circ$ (kcal/mol)	$-\Delta S_T^\circ$ (cal/mol K)	$-\Delta H_0^\circ$ (kcal/mol)	T[a]	D_e (kcal/mol)	D_o (kcal/mol)
1	39.6 ± 2.0	26.0 ± 3	39.2 ± 3.0	720–800	35.98	35.02
2	33.3 ± 0.8	29.9 ± 3	32.9 ± 1.5	555–745	28.56	27.30
3	13.7 ± 0.8	27.7 ± 2	13.3 ± 1.0	275–425	8.56	7.62
4	7.3 ± 0.7	22.9 ± 3	7.0 ± 1.0	175–275	2.51	2.04
5	3.0 ± 0.6	13.3 ± 3	3.0 ± 0.8	145–175	–	–

[a] Temperature range over which equilibrium data was acquired, in kelvin.

alkene ligands values ranged from approximately −20 to −30 cal/(mol K). The additions of subsequent ligands result in values of ΔS_T° that are approximately 10 entropy unit "less negative" than that of the fourth ligand addition.

In all cases, DFT calculations yielded theoretical binding energies in good agreement with experiment for addition of the first two ligands in all systems studied. The agreement is slightly worse for subsequent ligands, but the drop in binding energy is quantitatively duplicated. Additionally, theoretical molecular geometries and electronic population analysis, acquired from DFT, provided information necessary in order to elucidate the dominant bonding interaction of the various clusters.

5. Discussion

5.1. First alkene ligand additions

The first additions of C_2H_4 and C_3H_6 to Ag^+ and Ag_2^+ serve as effective prototypes for the analysis of the all the silver–alkene clusters discussed in this work. The relatively large BDEs of the first clusters suggest that covalent bonding is involved. Calculations show that a substantial amount of electron density, ranging from 0.11 to 0.20 electrons, is donated from the first alkene ligand to the transition metal center, supporting covalent bonding. The charge transfer is consistent with the fact that both ethene and propene are considered to be good electron donors. Electron donation is slightly larger for C_3H_6 than for C_2H_4, indicating a stronger covalent interaction could be involved. However, C_3H_6 has both a larger polarizability than C_2H_4 (6.3 versus 4.3 Å^3) [47] and dipole moment (0.44 versus 0.0 Da according to DFT) indicating electrostatic forces should also contribute to the differences in the observed binding energies.

A more extensive understanding of the bonding interactions of the first clusters can be gained by analysis of the valence electronic configuration of the species that participate in the bonding. The Ag^+ ion has a $4d^{10}5s^0$ valence electron configuration, which suggests that the majority of the charge donation to Ag^+ is to the unoccupied 5s-orbital since the 4d-orbitals are fully occupied and the 5p-orbitals lie much higher in energy. Similarly, the Ag_2^+ ion has a $(4d^{20}\sigma(5s)^1)$ valence electron configuration that suggests electron donation to the singly occupied σ(5s)-orbital. The highest occupied molecular orbital (HOMO) of C_2H_4 and C_3H_6 is the $\pi(2p_y)^2$ bonding orbital that makes up the C–C double bond in both molecules. This suggests that donation to the 5s-orbital of Ag^+ and the σ(5s)-orbital of Ag_2^+ should originate from the $\pi(2p_y)^2$-orbital, a bonding scheme consistent with the metal–olefin bonding model proposed by Dewar [38]. Indeed, our NBO population analysis [48] shows that the dominant bond interaction is donation from the $\pi(2p_y)^2$-orbital of the alkene ligands to the 5s-orbital of Ag^+ and the σ(5s)-orbital of Ag_2^+ (see Table 5). However, NBO also shows that the populations of the 4d-orbitals of Ag^+ and Ag_2^+ remain mostly unchanged when bound to the alkene ligands, indicating that back-donation from the 4d-orbitals to the $\pi^*(2p_y)$ antibonding orbital of the alkenes is minimal and does not play a large role in the silver–alkene bond interaction.

Both C_2H_4 and C_3H_6 adsorb side-on to Ag^+ and Ag_2^+, perpendicular to the silver–alkene bond axis (see Figs. 5–8). This orientation allows for electron donation from the $\pi(2p_y)^2$-orbital to occur because these orbitals lie above and below the plane of the alkene molecules. Additionally, the calculated C–C bond distance for the first clusters is increased slightly

Table 4
Data summary for $Ag_2^+(C_3H_6)_{n-1} + C_3H_6 \rightleftarrows Ag_2^+(C_3H_6)_n$

n	Experiment				Theory	
	$-\Delta H_T^\circ$ (kcal/mol)	$-\Delta S_T^\circ$ (cal/mol K)	$-\Delta H_0^\circ$ (kcal/mol)	T[a]	D_e (kcal/mol)	D_o (kcal/mol)
1	28.5 ± 0.8	21.9 ± 2	28.1 ± 1.5	700–800	24.54	23.52
2	25.9 ± 0.8	24.3 ± 2	25.8 ± 1.5	625–720	18.43	17.48
3	12.5 ± 0.5	24.1 ± 2	12.4 ± 0.8	260–355	8.33	7.48
4	9.4 ± 0.3	27.2 ± 1	9.3 ± 0.5	200–300	4.84	4.34
5	4.4 ± 0.4	18.4 ± 2	4.4 ± 0.6	145–175	–	–

[a] Temperature range over which equilibrium data was acquired, in kelvin.

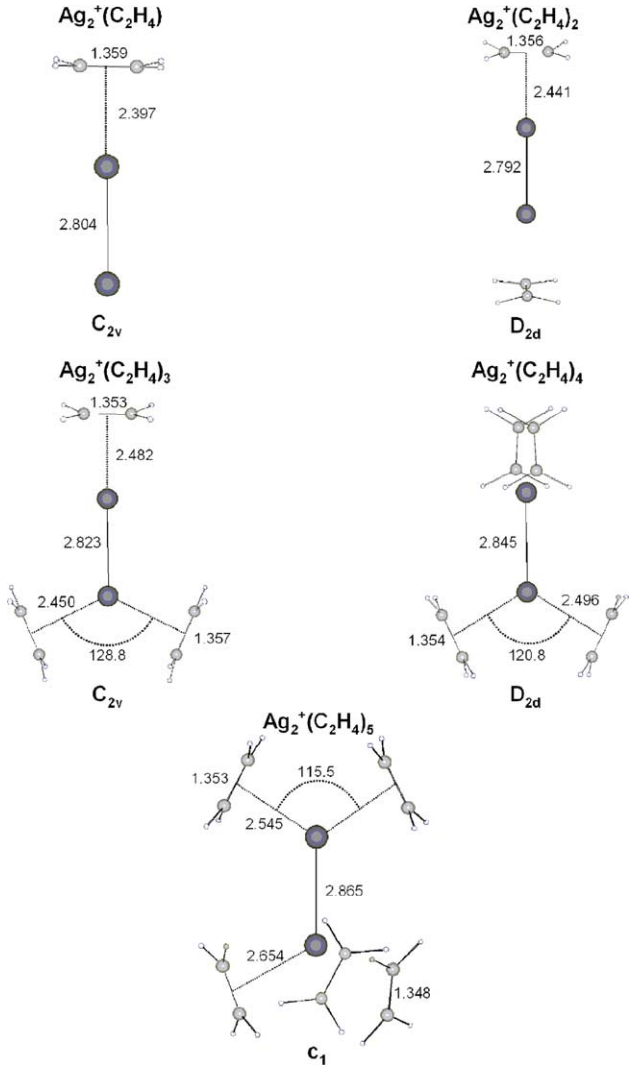

Fig. 6. Theoretical geometries of the $Ag_2^+(C_2H_4)_n$ clusters calculated at the DFT B3LYP level. Distances are in angstroms and angles in degrees. The *z*-axis is taken as the Ag_2^+—C_2H_4 bonding axis. All Ag_2^+—C_2H_4 bond distances are measured from the bonding atom of the Ag_2^+ ion to the center of the C—C double bond.

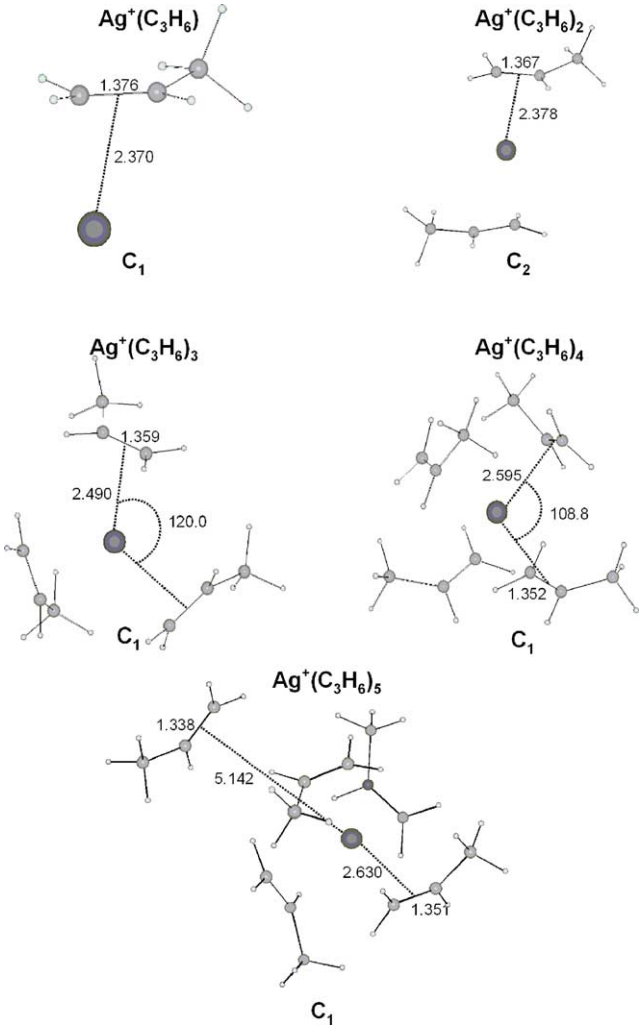

Fig. 7. Theoretical geometries of the $Ag^+(C_3H_6)_n$ clusters calculated at the DFT B3LYP level. Distances are in angstroms and angles in degrees. The *z*-axis is taken as the Ag^+—C_3H_6 bonding axis. All Ag^+—C_3H_6 bond distances are measured from the Ag^+ ion to the center of the C—C double bond.

compared to that of free the molecules (0.032 and 0.025 Å for $Ag_m^+(C_2H_4)$, $m = 1$ and 2, respectively, and 0.040 and 0.031 Å for $Ag_m^+(C_3H_6)$, $m = 1$ and 2, respectively), consistent with electron transfer out of a bonding orbital.

Although the bonding interactions of Ag^+ and Ag_2^+ with the first C_2H_4 and C_3H_6 ligands are similar, differences exist. Specifically, when the $Ag_2^+(L)$ clusters are compared to the analogous $Ag^+(L)$ clusters, we find: (1) reduced BDEs for the $Ag_2^+(L)$ clusters, (2) transition metal ion–ligand bond distances are increased, and (3) the C–C double bond distances are closer to the values calculated for an unbound C_2H_4 or C_3H_6 molecule. These phenomena have been observed in other transition metal dimer systems [12,19] and can be attributed to a reduction in the covalent interaction between the ligand and the transition metal dimer relative to the monomer. This reduction is caused by single electron occupation of the

Table 5
Natural bond order populations of $Ag_{1,2}^+(L)$ clusters

	Population	
	5s/σ(5s) (charge)[a]	π($2p_y$)
$Ag^+(C_2H_4)$	0.17 (0.88)	1.84
$Ag^+(C_2H_4)_2$[b]	0.35 (0.77)	1.85
$Ag_2^+(C_2H_4)$	1.13 (0.90)	1.86
$Ag_2^+(C_2H_4)_2$[b]	1.24 (0.83)	1.88
$Ag^+(C_3H_6)$	0.20 (0.85)	1.81
$Ag^+(C_3H_6)_2$[b]	0.37 (0.74)	1.84
$Ag_2^+(C_3H_6)$	1.16 (0.88)	1.84
$Ag_2^+(C_3H_6)_2$[b]	1.26 (0.81)	1.86
Ag^+	0.00 (1.00)	–
Ag_2^+	1.00 (1.00)	–
C_2H_4/C_3H_6	–	2.00

[a] Natural charges taken for NBO population analysis.

[b] 5s/σ(5s) populations are for *two ligands* donating electron density into the orbital. π($2p_y$) populations are for both ligands that donate equal amounts of electron density to a given metal center.

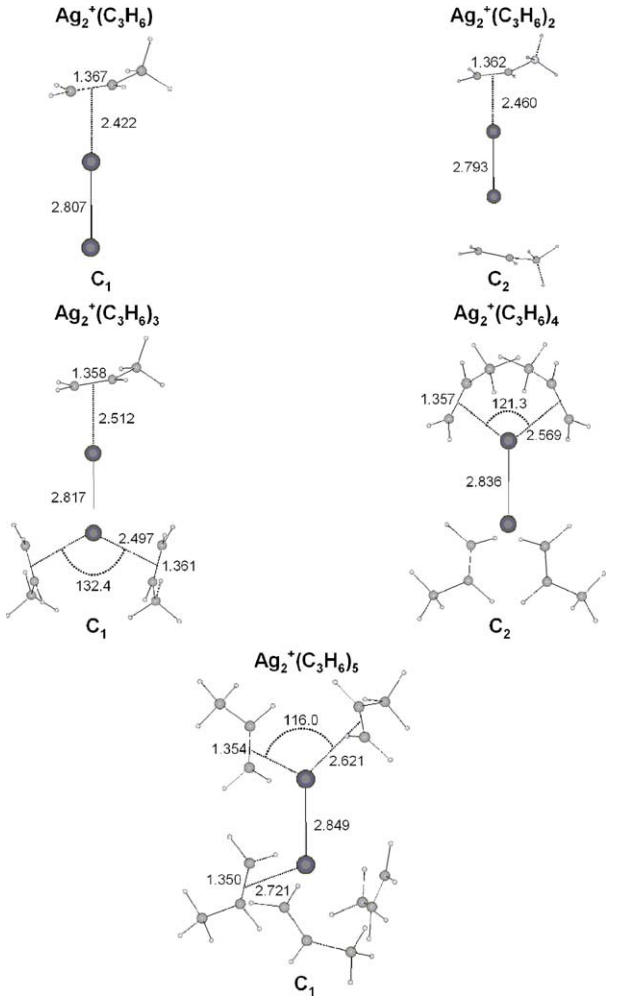

Fig. 8. Theoretical geometries of the $Ag_2^+(C_3H_6)_n$ clusters calculated at the DFT B3LYP level. Distances are in angstroms and angles in degrees. The z-axis is taken as the Ag_2^+—C_3H_6 bonding axis. All Ag_2^+—C_3H_6 bond distances are measured from the bonding atom of the Ag_2^+ ion to the center of the C—C double bond.

σ(5s)-orbital that forms the bond between $Ag(4d^{10}5s^1)$ and $Ag^+(4d^{10}5s^0)$, leading to increased on-axis Pauli repulsion with the ligand. Calculations show that the σ(5s) electron density of Ag_2^+ is polarized away from the alkene ligand. The cost of polarizing electron density away from the ligand coupled with increased on-axis Pauli repulsion and reduced $\pi(2p_y)^2$ donation to Ag_2^+ result in reduced bond strength and increased bond length in $Ag_2^+(C_2H_4)$ and $Ag_2^+(C_3H_6)$ relative to $Ag^+(C_2H_4)$ and $Ag^+(C_3H_6)$.

5.2. Second alkene ligand additions

The bonding interactions of the second ligand attachments are similar to the first, with $\pi(2p_y)^2$ donation from the alkene ligands to either the 5s-orbital of Ag^+ or the σ(5s)-orbital of Ag_2^+ (Table 5). NBO shows a substantial amount of electron donation from the alkene ligands to the transition metal core ions indicating that the bonding interactions of second clusters remain covalent in nature. However, NBO does show that there is a slight reduction in the average amount of $\pi(2p_y)^2$ electron density donated from the alkene ligands to the transition metal ions. This slightly reduced amount of electron transfer is likely the cause of the small decrease in BDE for the second alkene ligand additions as compared to the first.

NBO also provides some addition information that can be used to rationalize the reduced BDEs of second alkene ligand additions to the dimer. The decrease in BDE can again be attributed to the single occupation of the σ(5s)-orbital of Ag_2^+. Here, repulsive σ(5s) electron density is initially polarized away from the first alkene ligand. Consequentially, addition of the second ligand must now occur in an area of relatively high electron density. In order to reduce the amount of on-axis repulsion experienced by the second ligand, σ(5s) electron density is "repolarized" to near its original distribution in the bare Ag_2^+ core ion. The effect of this process is a decrease in the overall bond strength of the $Ag_2^+(L)_2$ clusters.

5.3. Third and fourth alkene ligand additions

The bonding interactions of both the third and fourth additions resemble those of the smaller clusters with electron density being donated from the $\pi(2p_y)^2$-orbitals of the alkene ligands to either the 5s-orbital of Ag^+ or the σ(5s)-orbital of Ag_2^+. The reduction in BDE from the second to third and fourth clusters can largely be attributed to a reduction in the covalent interactions between the transition metal core ion and the alkene ligands. NBO illustrates that electron donation is reduced in the third clusters compared to that of the second clusters and that the trend of reduced covalency continues for the fourth additions. The decreased metal ion–ligand interactions of the third and fourth clusters can be seen in their calculated molecular geometries (Figs. 5–8). The silver–alkene bond lengths of the third and fourth clusters have considerably increased compared to those of the first and second clusters. At the same time, the C–C bond distances of the carbon atoms sharing a double bond in the alkene ligands have decreased, shifting closer to the bond distances calculated for an unbound C_2H_4 or C_3H_6 molecule. These trends indicate reduced metal–ligand interactions for third and fourth clusters.

5.4. Fifth and sixth alkene ligand additions

Equilibrium for the fifth clusters of all the systems studied could only be observed over a very limited temperature range. In all cases, a large increase in association entropy is observed for the addition of the fifth alkene ligand, indicating this ligand is much more mobile than the first four and hence occupies the second solvation shell. DFT calculations are consistent with this observation. All of the calculated fifth cluster binding energies (D_o) are approximately 0 kcal/mol, indicating that the fifth ligand is essentially unbound. This is not an uncommon DFT result for ligand addition in the

second solvation shell. The theoretical Ag^+–alkene bond distances for the fifth ligands are greater than 5 Å, while the bond distances from Ag^+ to the other four alkene ligands remain nearly unchanged. The C–C double bond distance of the fifth alkene ligands are approximately the same as that calculated for either a free C_2H_4 or C_3H_6 molecule. The DFT minimum energy structures for the Ag_2^+–alkene fifth clusters yield bond distances shorter than the analogous Ag^+ systems, even though the predicted binding energies are near zero.

Data for a sixth alkene ligand addition, $Ag^+(C_2H_4)_6$, was obtained at 115 K. A BDE of 3.3 kcal/mol for $Ag^+(C_2H_4)_6$ was estimated by assuming an association entropy equal to that of the $Ag^+(C_2H_4)_5$ cluster. The theoretical binding energy for $Ag^+(C_2H_4)_6$ suggests that the sixth C_2H_4 ligand is essentially unbound with respect to the separated reactants ($Ag^+(C_2H_4)_5 + C_2H_4$). The calculated geometry of the sixth cluster also shows a long bond distance from Ag^+ to the sixth C_2H_4 ligand (5.423 Å) and a C–C bond distance nearly equal to that of free C_2H_4.

6. Conclusions

1. Bond dissociation energies and association entropies were determined for sequential clustering of up to six C_2H_4 and C_3H_6 ligands to the Ag^+ and Ag_2^+ ions. The ligands attach with the first two strongly bound, the next two more weakly bound and the last two very weakly bound. Analysis of the entropies of association indicate the first four ligands form the first solvation shell and subsequent ligands begin to fill a second solvation shell.
2. Density functional theory calculations (B3LYP parameterization) yielded bond dissociation energies in good agreement with experiment for addition of the first two ligands in all systems studied. The agreement is slightly worse for subsequent ligands, but the drop in binding energy observed experimentally is quantitatively duplicated.
3. DFT calculations indicate the first solvation shell is filled with four ligands in agreement with experimentally measured association entropies.
4. The addition of the first two ligands bonding with the transition metal center has a strong covalent character exemplified by electron donation from the $\pi(2p_y)^2$-orbital of the ligands into the unoccupied 5s-orbital of Ag^+ or the singly occupied $\sigma(5s)$-orbital of Ag_2^+. As additional ligands are added, the bonding takes on more electrostatic character. The bonding for the fifth (and sixth) ligand is essentially purely electrostatic (second solvation shell).

Acknowledgements

The support of the Air Force Office of Scientific Research under grants F 49620-01-1-0459 and F 49620-03-1-0046 is gratefully acknowledged. M.J.M. would also like to thank C.J. Carpenter for helpful input regarding the preparation of this manuscript.

References

[1] M.B. Knickelbein, Annu. Rev. Phys. Chem. 50 (1999) 79.
[2] P.R. Kemper, J. Bushnell, G. von Helden, M.T. Bowers, J. Phys. Chem. 97 (1993) 52.
[3] P.R. Kemper, J. Bushnell, P. van Koppen, M.T. Bowers, J. Phys. Chem. 97 (1993) 1810.
[4] J.E. Bushnell, P.R. Kemper, M.T. Bowers, J. Phys. Chem. 97 (1993) 11628.
[5] J.E. Bushnell, P.R. Kemper, P. Maitre, M.T. Bowers, J. Am. Chem. Soc. 116 (1994) 9710.
[6] J.E. Bushnell, P.R. Kemper, M.T. Bowers, J. Phys. Chem. 99 (1995) 15602.
[7] P.R. Kemper, P. Weis, M.T. Bowers, Int. J. Mass Spectrom. Ion Process. 160 (1997) 17.
[8] P. Weis, P.R. Kemper, M.T. Bowers, J. Phys. Chem. A 101 (1997) 2809.
[9] J.E. Bushnell, P. Maitre, P.R. Kemper, M.T. Bowers, J. Chem. Phys. 106 (1997) 10153.
[10] P.R. Kemper, P. Weis, M.T. Bowers, Chem. Phys. Lett. 293 (1998) 503.
[11] P.R. Kemper, P. Weis, M.T. Bowers, P. Maitre, J. Am. Chem. Soc. 120 (1998) 13494.
[12] M.J. Manard, J.E. Bushnell, S.L. Bernstein, M.T. Bowers, J. Phys. Chem. A 106 (2002) 10027.
[13] M.R. Sievers, P.B. Armentrout, J. Phys. Chem. 99 (1995) 8135.
[14] F.A. Khan, D.E. Clemmer, R.H. Schultz, P.B. Armentrout, J. Phys. Chem. 97 (1993) 7978.
[15] R.H. Schultz, K.C. Crellin, P.B. Armentrout, J. Am. Chem. Soc. 113 (1991) 8590.
[16] S. Goebel, C.L. Haynes, F.A. Khan, P.B. Armentrout, J. Am. Chem. Soc. 117 (1995) 6994.
[17] F.A. Khan, D.L. Steele, P.B. Armentrout, J. Phys. Chem. 99 (1995) 7819.
[18] F. Meyer, Y.M. Chen, P.B. Armentrout, J. Am. Chem. Soc. 117 (1995) 4071.
[19] M.J. Manard, P.R. Kemper, M.T. Bowers, Int. J. Mass Spectrom. 228 (2003) 865.
[20] (a) D. Vardhan, R. Liyanage, P.B. Armentrout, J. Chem. Phys. 119 (2003) 4166;
(b) X.G. Zhang, P.B. Armentrout, J. Phys. Chem. A 107 (2003) 8904.
[21] P.A.M. van Koppen, P.R. Kemper, J.E. Bushnell, M.T. Bowers, J. Am. Chem. Soc. 117 (1995) 2098.
[22] Q. Zhang, P.R. Kemper, S.K. Shin, M.T. Bowers, Int. J. Mass Spectrom. 204 (2001) 281.
[23] Q. Zhang, P.R. Kemper, M.T. Bowers, Int. J. Mass Spectrom. 210 (2001) 265.
[24] P.A.M. van Koppen, J.K. Perry, P.R. Kemper, J.E. Bushnell, M.T. Bowers, Int. J. Mass Spectrom. 187 (1999) 989.
[25] P.R. Kemper, M.T. Hsu, M.T. Bowers, J. Phys. Chem. 95 (1991) 10600.
[26] J.E. Bushnell, P.R. Kemper, M.T. Bowers, J. Phys. Chem. 98 (1994) 2044.
[27] P.R. Kemper, J. Bushnell, M.T. Bowers, G.I. Gellene, J. Phys. Chem. A 102 (1998) 8590.
[28] P.A.M. van Koppen, M.T. Bowers, C.L. Haynes, P.B. Armentrout, J. Am. Chem. Soc. 120 (1998) 5704.
[29] P. Weis, P.R. Kemper, M.T. Bowers, J. Phys. Chem. A 101 (1997) 8207.
[30] (a) J.G. Serafin, A.C. Liu, S.R. Seyedmonir, J. Mol. Catal. A: Chem. 131 (1998) 157;
(b) D.J. Sajkowski, M. Boudart, Catal Rev. 29 (1987) 325;
(c) A.L. de Oliveira, A. Wolf, F. Schuth, Catal. Lett. 73 (2001) 157.
[31] Y.M. Chen, P.B. Armentrout, J. Phys. Chem. 99 (1995) 11424.
[32] B.C. Guo, A.W. Castleman, Chem. Phys. Lett. 181 (1991) 16.

[33] J. Kaneti, L.C.P.M. de Smet, R. Boom, H. Zuilhof, E.J.R. Sudholter, J. Phys. Chem. A 106 (2002) 11197.
[34] Y.C. Huang, P.H. Su, C.S. Yeh, B Chem. Soc. Jpn. 74 (2001) 677.
[35] R.H. Hertwig, W. Koch, D. Schroder, H. Schwarz, J. Hrusak, P. Schwerdtfeger, J. Phys. Chem. 100 (1996) 12253.
[36] N.L. Ma, Chem. Phys. Lett. 297 (1998) 230.
[37] T. Ziegler, A. Rauk, Inorg. Chem. 18 (1979) 1558.
[38] J.S. Dewar, B Soc. Chim. Fr. 18 (1951) 71.
[39] P.R. Kemper, M.T. Bowers, J. Am. Soc. Mass Spectrom. 1 (1990) 197.
[40] (a) P. Hohenberg, W. Kohn, Phys. Rev. B 136 (1964) 864;
(b) W. Kohn, L.J. Sham, Phys. Rev. 140 (1965) 1133.
[41] P.J. Stephens, F.J. Devlin, C.F. Chabalowski, M.J. Frisch, J. Phys. Chem. 98 (1994) 11623.
[42] (a) A.D. Becke, J. Chem. Phys. 98 (1993) 5648;
(b) A.D. Becke, Phys. Rev. A 38 (1988) 3098.
[43] M.J. Frisch, G.W. Trucks, H.B. Schlegel, G.E. Scuseria, M.A. Robb, J.R. Cheeseman, V.G. Zakrzewski, J. Montgomery, R.E. Stratmann, J.C. Burant, S. Dapprich, J.M. Millam, A.D. Daniels, K.N. Kudin, M.C. Strain, O. Farkas, J. Tomasi, V. Barone, M. Cossi, R. Cammi, B. Mennucci, C. Pomelli, C. Adamo, S. Clifford, J. Ochterski, G.A. Petersson, P.Y. Ayala, Q. Cui, K. Morokuma, D.K. Malick, A.D. Rabuck, K. Raghavachari, J.B. Foresman, J. Cioslowski, J.V. Ortiz, A.G. Baboul, B.B. Stefanov, G. Liu, A. Liashenko, P. Piskorz, I. Komaromi, R. Gomperts, R.L. Martin, D.J. Fox, T. Keith, M.A. Al-Laham, C.Y. Peng, A. Nanayakkara, C. Gonzalez, M. Challacombe, P.M.W. Gill, B. Johnson, W. Chen, M.W. Wong, J.L. Andres, C. Gonzalez, M. Head-Gordon, E.S. Replogle, J.A. Pople, Pittsburgh, PA, 1998.
[44] (a) M.M. Francl, W.J. Pietro, W.J. Hehre, J.S. Binkley, M.S. Gordon, D.J. Defrees, J.A. Pople, J. Chem. Phys. 77 (1982) 3654;
(b) T. Clark, J. Chandrasekhar, G.W. Spitznagel, P.V. Schleyer, J. Comput. Chem. 4 (1983) 294;
(c) R. Krishnan, J.S. Binkley, R. Seeger, J.A. Pople, J. Chem. Phys. 72 (1980) 650;
(d) P.M.W. Gill, B.G. Johnson, J.A. Pople, M.J. Frisch, Chem. Phys. Lett. 197 (1992) 499.
[45] (a) P.J. Hay, W.R. Wadt, J. Chem. Phys. 82 (1985) 270;
(b) W.R. Wadt, P.J. Hay, J. Chem. Phys. 82 (1985) 284;
(c) P.J. Hay, W.R. Wadt, J. Chem. Phys. 82 (1985) 299.
[46] Basis sets were obtained from the Extensible Computational Chemistry Environment Basis Set Database, Version 10/21/03, as developed and distributed by the Molecular Science Computing Facility, Environmental and Molecular Sciences Laboratory which is part of the Pacific Northwest Laboratory, P.O. Box 999, Richland, Washington 99352, USA, and funded by the U.S. Department of Energy. The Pacific Northwest Laboratory is a multi-program laboratory operated by Battelle Memorial Institute for the U.S. Department of Energy under contract DE-AC06-76RLO 1830. Contact David Feller or Karen Schuchardt for further information.
[47] H. Nishimura, H. Tawara, J. Phys. B: At. Mol. Opt. Phys. 27 (1994) 2063.
[48] A.E. Reed, L.A. Curtis, F. Weinhold, Chem. Rev. 88 (1988) 899, and references therein.